ORIGINAL PAPER

Volume and neuron number of the lateral geniculate nucleus in schizophrenia and mood disorders

**Karl-Anton Dorph-Petersen · Damira Caric ·
Ramin Saghafi · Wei Zhang · Allan R. Sampson ·
David A. Lewis**

Abstract Subjects with schizophrenia show deficits in visual perception that suggest changes predominantly in the magnocellular pathway and/or the dorsal visual stream important for visiospatial perception. We previously found a substantial 25% reduction in neuron number of the primary visual cortex (Brodmann's area 17, BA17) in postmortem tissue from subjects with schizophrenia. Also, many studies have found reduced volume and neuron number of the pulvinar—the large thalamic association nucleus involved in higher-order visual processing. Here, we investigate if the lateral geniculate nucleus (LGN), the visual relay nucleus of the thalamus, has structural changes in schizophrenia. We used stereological methods based on unbiased principles of sampling (Cavalieri's principle and the optical fractionator) to estimate the total volume and neuron number of the magno- and parovocellular parts of the left LGN in postmortem brains from nine subjects with schizophrenia, seven matched normal comparison subjects and 13 subjects with mood disorders. No significant schizophrenia-related structural differences in volume or neuron number of the left LGN or its major subregions were found, but we did observe a significantly increased total volume of the LGN, and of the parvocellular lamina and interlaminar regions, in the mood group. These findings do not support the hypothesis that subjects with schizophrenia have structural changes in the LGN. Therefore, our previous observation of a schizophrenia-related reduction of the primary visual cortex is probably not secondary to a reduction in the LGN.

Keywords Stereology · Cell count · Schizophrenia · Mood disorders · Lateral geniculate body

K.-A. Dorph-Petersen · D. Caric · R. Saghafi · D. A. Lewis
Department of Psychiatry, University of Pittsburgh,
Pittsburgh, PA 15213, USA

W. Zhang · A. R. Sampson
Department of Statistics, University of Pittsburgh, Pittsburgh,
PA 15213, USA

D. A. Lewis
Department of Neuroscience, University of Pittsburgh,
Pittsburgh, PA 15213, USA

K.-A. Dorph-Petersen (✉)
Centre for Psychiatric Research,
Aarhus University Hospital, Risskov,
Skovagervej 2, 8240 Risskov, Denmark
e-mail: Karl-Anton@Dorph-Petersen.dk

D. Caric
Department of Psychiatry, Allegheny General Hospital,
Pittsburgh, PA 15212, USA

Introduction

An increasing number of studies document that subjects with schizophrenia have subtle impairments in visual perception—see [14] for a recent review. Many studies have reported early perceptional changes selective to or predominantly in the magnocellular pathway/dorsal stream—see [15, 16, 23, 48, 53] and references therein, although the system specificity has been questioned [71], and involvement of the parvocellular system has been seen [72]. The *magnocellular pathway* conveys visual information from the M cells of the retina via the magnocellular laminae of

the lateral geniculate nucleus (LGN) of the thalamus to the primary visual cortex (Brodmann's area 17, BA17) and then predominantly via the *dorsal stream* into visual areas of parieto-occipital cortex. The *parvocellular pathway* conveys visual information from the P cells of the retina via the parvocellular laminae of the LGN to BA17 and subsequently predominantly via the *ventral stream* into visual areas of the temporo-occipital cortex [56, 57]. The magnocellular pathway/dorsal stream is selective for perception of motion and position (the '*where*' stream), while the parvocellular pathway/ventral stream is selective for perception of color and shape (the '*what*' stream) [58, 78]. For reviews see also [20, 79]. Thus, the observed impairments of the visual system in schizophrenia appear to predominantly involve visiospatial perception and only to a lesser degree object recognition.

In support of the physiological and behavioral findings described above, several functional imaging studies of subjects with schizophrenia have reported changes in primary visual cortex activity [5, 26]. In addition, diffusion tensor imaging MRI studies have reported reduced white matter integrity in the optic radiations bilaterally in subjects with schizophrenia [8, 13, 16]—see also [7].

In a recent postmortem study of subjects with schizophrenia we found a marked reduction in neuron number (25%) and total volume (22%) of BA17 without any change in neuronal density or cortical thickness [30]. In contrast, two postmortem studies of the LGN did not find any schizophrenia-related changes in total volume of the nucleus [54] or in cell numbers [64]. Here, we further investigate the potential role of the LGN in the pathology of schizophrenia. We used methods based upon unbiased stereological principles to assess the total volumes and neuron numbers of the magnocellular and/or parvocellular regions of the LGN in subjects with schizophrenia, normal comparison subjects, and subjects with mood disorders. The latter group was included to test the diagnostic specificity of any findings in the schizophrenia group.

In light of the previous findings, we sought to test the following hypotheses: (1) the schizophrenia group has a smaller total volume and/or number of neurons of the LGN compared to both controls and the mood group. (2) Such changes in the schizophrenia group involve the magnocellular laminae of the LGN more than the parvocellular laminae.

Subjects and methods

Subjects

The current study is based upon a convenience sample of tissue sections from our previous study of the mediodorsal

(MD) thalamic nucleus [29] which includes further details and discussion of the subject selection. Because a substantial proportion of subjects with schizophrenia also suffer from comorbid mood and/or alcohol and/or drug related disorders [32, 70], excluding subjects with these comorbidities would have resulted in a non-representative sample. Consequently, in order to assess the diagnostic specificity of findings in such a representative but heterogeneous group of subjects, we included a second comparison group without schizophrenia but with a comparable load of comorbidities. Thus, we studied three diagnostic groups: subjects with schizophrenia, normal comparison subjects, and a heterogeneous group of subjects with mood disorders some of whom had alcohol and/or substance-related disorders. It should be emphasized that the latter group was included to test the diagnostic specificity of any findings in the schizophrenia group and not intended as a separate study group of mood disorders.

Brain specimens from 38 subjects were obtained from autopsies conducted at the Allegheny County Medical Examiner's Office, with the consent of the next-of-kin and the approval of the Health Sciences Institutional Review Board of the University of Pittsburgh. Consensus DSM-IV diagnoses [3] for each subject were made using information obtained from medical records and/or structured interviews conducted with family members as previously described [29].

Nine of the 38 subjects had to be excluded because the complete LGN was not preserved in the final histological slides (see tissue preparation). Thus, the final subject sample consisted of nine subjects with schizophrenia, seven normal comparison subjects and 13 subjects with mood disorders. The subject groups were similar in sex, age, and postmortem interval (Table 1). The postmortem interval was defined as the time between the estimated time of death and the time when the brain was placed in ice-cold 4% paraformaldehyde. Note that three brains excluded in our previous study of the MD contained the complete LGN and were therefore included here. Two subjects (697 and 816) had a history of eye trauma and eye surgery, respectively, but both events were expected to be too subtle to induce changes in the structural parameters of the LGN assessed in this study. Gross and microscopic neuropathological screening revealed no abnormalities in any of the 29 subjects except as follows: three subjects (803, 843, and 871) experienced blunt force trauma to the head that resulted in intracranial hemorrhages and two subjects (602 and 699) died of a self-inflicted gunshot wound to the head. All of these injuries were acute and no damage to the thalamus was observable.

The normal comparison, schizophrenia, and mood disorder subject groups did not differ significantly $(F_{2,26} < 1.4; P > 0.26)$ in mean age or postmortem interval

Table 1 Demographics of the subjects included in this study

Case	Diagnosis	Sex/race	Age (years)	Brain weight (kg)	PMI[a] (h)	Strg time[b] (months)	Cause of death[c]
Normal comparison subjects							
568	Comparison subject	F/W	60	1.345	9.5	61.4	ASCVD
634	Comparison subject	M/W	52	1.620	16.2	51.9	ASCVD
686	Comparison subject	F/W	52	1.240	22.6	44.7	ASCVD
700	Comparison subject	M/W	42	1.670	26.1	45.0	ASCVD
794	Comparison subject	M/B	52	1.255	20.0	26.6	Cardiomyopathy
795	Comparison subject	M/W	68	1.400	12.0	25.5	Ruptured abdominal aortic aneurysm
871	Comparison subject	M/W	28	1.440	16.5	13.0	Trauma
Mean			50.6	1.424	17.6	38.3	
CV*			0.25	0.12	0.33	0.45	
Subjects with schizophrenia							
466	Chronic undifferentiated schizophrenia	M/B	48	1.270	19.0	81.0	ASCVD
640	Chronic paranoid schizophrenia	M/W	49	1.260	5.2	49.2	Pulmonary embolism
656	Schizoaffective disorder[d]	F/B	47	1.350	20.1	48.1	Suicide by gun shot
829	Schizoaffective disorder[d,i,j]	M/W	25	1.160	5.0	17.6	Suicide by drug overdose
843	Chronic disorganized schizophrenia	F/W	41	1.490	17.1	16.6	Suicide by jumping
878	Disorganized schizophrenia[d]	M/W	33	1.385	10.8	10.5	Myocardial fibrosis
900	Chronic paranoid schizophrenia	M/B	56	1.570	12.3	12.0	ASCVD
904	Schizoaffective disorder	M/W	33	1.565	29.0	7.1	Bronchopneumonia
917	Chronic undifferentiated schizophrenia	F/W	71	1.150	23.8	7.4	ASCVD
Mean			44.8	1.356	15.8	27.7	
CV*			0.31	0.12	0.52	0.93	
Subjects with mood disorders							
203	Bipolar disorder with psychotic features[f,k]	F/W	70	1.370	19.3	132.3	ASCVD
505	Major depression[d]	M/W	57	1.440	12.8	68.6	Suicide by gun shot
564	Major depression with psychotic features	F/W	56	1.355	16.6	60.5	Suicide by hanging
602	Major depression[d]	M/W	56	1.375	11.8	54.8	Suicide by gun shot
652	Dysthymia, alcohol induced mood disorder[d]	M/W	44	1.385	21.9	48.9	Pneumonia
697	Bipolar disorder with psychotic features[k]	M/W	39	1.530	25.9	44.3	Suicide by exsanguinations
699	Major depression	M/W	65	1.435	5.5	42.7	Suicide by gunshot
735	Major depression[e,i]	F/W	40	1.385	14.0	36.7	Pulmonary thromboembolism
803	Major depression	F/W	65	1.265	18.0	25.6	Trauma
816	Major depression with psychotic features[k]	F/W	55	1.430	13.0	23.2	Myocardial fibrosis
834	Alcohol induced mood disorder[d]	M/W	50	1.350	9.5	22.9	Pneumonia
862	Major depression[d,g]	M/W	49	1.520	10.0	17.3	Upper GI bleed
868	Major depression[d,h]	M/W	47	1.530	10.5	16.7	Trauma
Mean			53.3	1.413	14.5	45.7	
CV*			0.18	0.06	0.39	0.68	

* Coefficient of variation CV = SD/mean

[a] PMI, postmortem interval in hours

[b] Storage time, tissue storage time at −30°C in months

[c] ASCVD, atherosclerotic coronary vascular disease

[d] Alcohol dependence, current at time of death

[e] Alcohol dependence, in remission at time of death

[f] Alcohol abuse, in remission at time of death

[g] Other substance dependence, in remission at time of death

[h] Other substance abuse, current at time of death

[i] Other substance abuse, in remission at time of death

[j] Schizophrenic subject off medications at time of death

[k] Psychiatric subjects with history of treatment with antipsychotic medications

(Table 1). The proportions of female subjects were 29, 33, and 38%, respectively; the proportions of Caucasian subjects were 86, 67, and 100%, respectively. Three of the subjects with schizophrenia and eight of the mood disorder subjects also had a history of alcohol or other substance-related disorders (Table 1).

Tissue preparation

The histological slides used in this study were generated as previously described [29]. In brief, for each brain the ventral part of the fresh left hemisphere was cut into coronal slices ∼15 mm thick. The slices were immersed in ice-cold 4% paraformaldehyde in phosphate buffer (pH = 7.3) for 48 h, washed in a graded series of sucrose solutions (12, 16, 18%), and then stored in an antifreeze solution (30 vol% ethylene glycol and 30 vol% glycerin in 0.024 M phosphate buffer) at −30°C. Tissue storage time did not differ significantly across the three subject groups (Table 1). For each subject, the thalamus—typically contained in 3–4 blocks—was removed with a rim of surrounding tissue, washed in 18% sucrose in PBS for 10–14 days to remove the antifreeze solution, and cut using a calibrated Microm HM500M cryostat (Microm, Germany). The blocks were cut exhaustively into coronal sections and a systematic uniformly random sample of one 80-μm-section per 640 μm was collected. Due to the unevenness of the block surfaces the first and last sections cut from each block were incomplete (i.e., did not cover the full block area). Because all sections, including the incomplete ones, were collected, and available for sampling, no bias was introduced. The sections were mounted on gelatin-coated glass slides, air-dried at room temperature overnight, and then stained for Nissl substance using thionin. The resulting final average section thickness was 23.5 μm (measured as a part of the stereological analysis described below), corresponding to 71% shrinkage in the z-axis of the sections. The notation "80-μm-sections" indicates that the sections were cut with a block advance $BA = 80$ μm as discussed by Dorph-Petersen et al. [27]. Sections were coded at the time of cryosectioning to keep the investigators blind to the diagnostic status of each subject. Two investigators (R.S., D.C.) who had not previously been exposed to the material performed all the stereological microscopy to further ensure full blindness in the current study.

Delineation of LGN

The distinctive architecture of the LGN [46] makes it easily identifiable in the ventrolateral portion of the caudal thalamus—even by the unaided eye. The rostral part of the LGN is located lateral to the medial geniculate nucleus and the caudal part is lateral to the inferior pulvinar nucleus, using the terminology of Hirai and Jones [44]. The LGN is almost surrounded by the fibers of the visual pathway—rostroventrally by the optic tract and dorsolaterally and caudally by the optic radiation. Ventrolaterally, the LGN is located just below the pial surface of the thalamus where it is visible as the characteristic knee-like protrusion leading to its name. Thus, the outermost cell dense laminae and their natural extensions clearly define the borders of the LGN (Fig. 1) and readily distinguish it from nearby structures. The human LGN shows the laminar pattern seen in most primates of two magnocellular laminae (1–2) with large neurons (Fig. 2a) and four parvocellular laminae (3–6) containing small to medium sized neurons (Fig. 2b). As seen in Fig. 1, lamina 3 and 5 form a continuum, and the same is true for lamina 4 and 6 (although the latter is not visible at the rostral–caudal level of Fig. 1). Intercalated between the neuron dense layers are the interlaminar regions sparsely populated by koniocellular neurons [41]. We frequently observed small islands of magnocellular neurons embedded in the parvocellular layers (Fig. 1). These islands, previously described by Hickey and Guillery [42], are easy to delineate and were regarded as part of the magnocellular compartment. In accordance with the literature on the human LGN [6, 42], the overall pattern of lamination was highly variable across subjects in our material. However, the caudal part of the human LGN has a generally less complex structure and more constant laminar arrangement than the rostral part [42]. Examining the LGN starting with caudal sections first allowed us to easily examine and recognize each layer in subsequent sections despite the more complex laminar arrangements in the rostral LGN.

In 18 of our subjects, the entire LGN was present in one thalamic block, whereas in the remaining 11 cases the LGN was contained in series of sections from two thalamic blocks. Thus, the LGN appeared in 9–16 of the Nissl stained coronal sections, including a few incomplete LGN sections at the transition between tissue blocs. All stained sections were used for the stereological analysis resulting in a section sampling fraction of 1/8, corresponding to one 80-μm section for every 640 μm.

Microscope setup

The histological sections from each subject were analyzed on an Olympus BX51 microscope equipped with a MT1201 microcator (0.2 μm resolution) and ND281B readout (Heidenhain, Germany), and a X–Y–Z motorized specimen stage (ProScan, Prior Scientific, UK). With a 2× photo eyepiece (PE2×, Olympus), a three-chip CCD camcorder (KY-F55B, JVC, Japan) was mounted on the top of the microscope and forwarded a 760 × 570 pixels live image (50 frames/s) to a personal computer. The
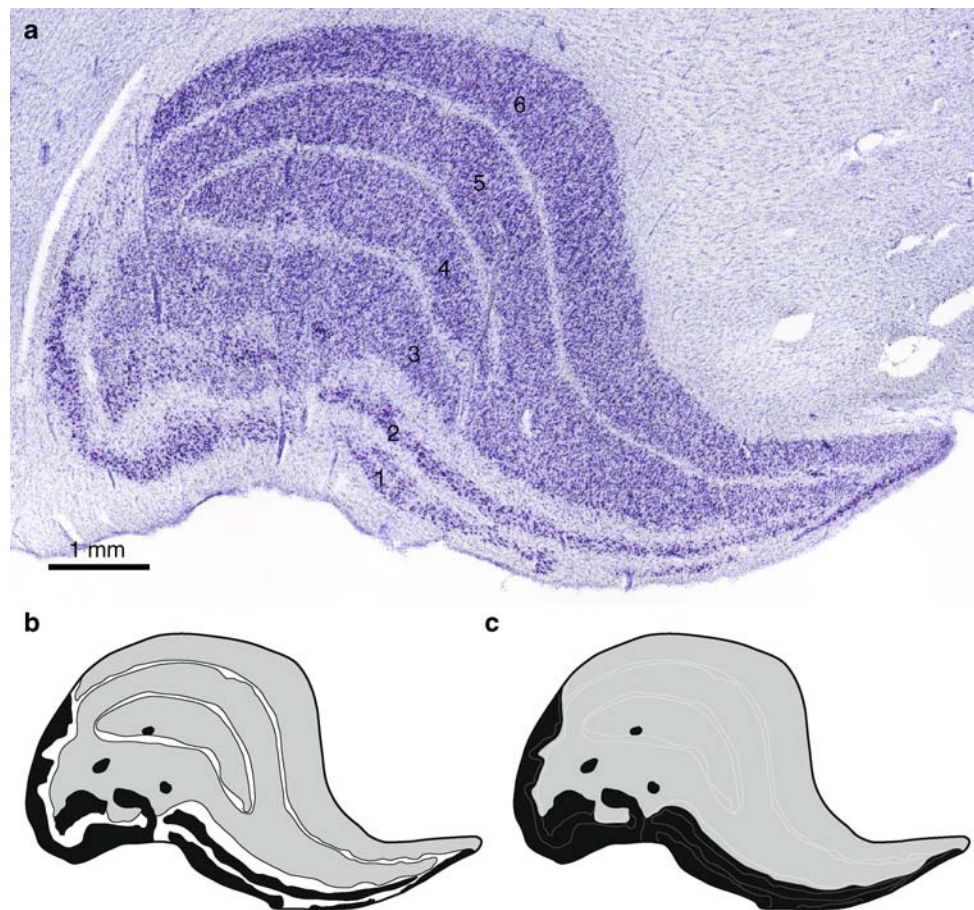
Fig. 1 a Coronal section approximately at the middle rostral–caudal level of the LGN. The six laminae are indicated. **b** For volume estimation, the LGN from each subject was subdivided into magnocellular laminae (*black*), parvocellular laminae (*gray*), and interlaminar regions (*white*). **c** For estimation of neuron numbers, the LGN from each subject was split into a magnocellular part (*black*) and a parvocellular part (*gray*)

computer ran the CAST stereology software package (Version 2.00.07, Olympus, Denmark) and was fitted with a frame grabber (Flashpoint 3D, Integral Technologies, IN) and a 19-in. monitor (FlexScan T765 Color Display Monitor, EIZO Nanao, Japan) having a screen resolution of 1,280 × 1,024 pixels. The microscope was mounted on a vibration isolation table (Q500A, Qontrol Devices Inc., CA, USA) to facilitate imaging at high magnification. Using an Olympus calibration slide, the system was calibrated daily for magnification, paracentricity of objectives and exact alignment of stage and camera.

Estimation of reference volume using Cavalieri's principle

For each subject we estimated the volumes of the three main compartments of the left LGN—(1) the magnocellular laminae, (2) the parvocellular laminae, and (3) the interlaminar regions (Fig. 1b). Using a 4× objective

(Olympus, UPlanApo, NA 0.16) resulting in a final on-screen magnification of 105×, the CAST software package superimposed a uniformly random integral rectangular point grid over each field of view. The point grid had two types of points with every ninth point encircled (Fig. 3). The CAST software allows—by manual stepping in x and y—the user to completely cover the region of interest with adjacent fields of view without the need of delineating the region in advance. A single investigator (R.S.) counted the number of points (P) in each section that hit the magnocellular laminae and the interlaminar regions, respectively, as well as the number of encircled points that hit the parvocellular laminae and the whole LGN, respectively. Points hitting the magnocellular islands embedded in the parvocellular laminae were included in the magnocellular point counts. Using Cavalieri's principle [39, 45], the volume (V) of each compartment as well as the total LGN was estimated for each set of sections as the product of the intersection distance ($T = 640 \mu m$), the relevant area per
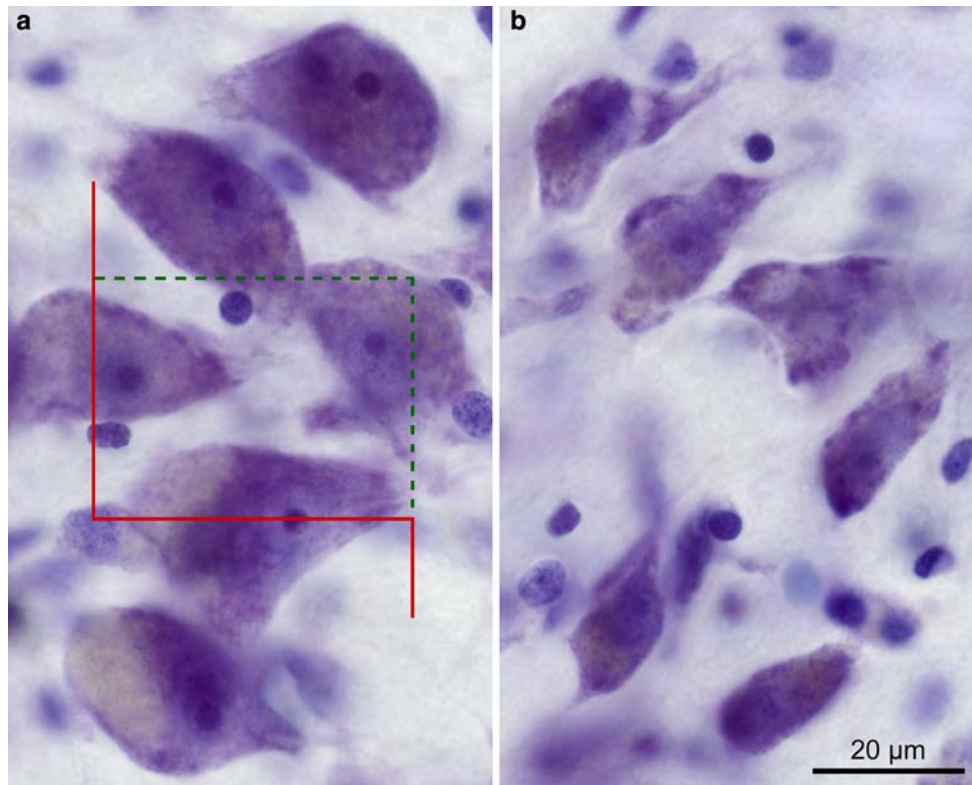
Fig. 2 a Micrograph showing six typical magnocellular neurons. An unbiased counting frame is shown with the *red* unbroken exclusion line and a *dotted green* inclusion line. A neuron was counted if its nucleolus was in focus within the height of the disector and fully or partially inside the counting frame without touching the exclusion line. As shown here, the two neurons in the middle were counted while the neurons just below and above the middle were excluded. **b** Six representative parvocellular neurons

point ($a = 0.0510$ mm^2, all points; or $a = 0.459$ mm^2, encircled points), and the respective sum of the number of counted points:

$$V := T \cdot a \cdot \sum P. \tag{1}$$

Here and elsewhere, := indicates that the quantity at left is estimated by the formula at the right. An average of 389 (219–557) magnocellular-points, 292 (179–353) parvocellular-points, 561 (257–1,010) interlaminar-points, and 396 (243–531) total-LGN-points were counted per subject in the set of 9–16 (mean: 12.8) sections containing LGN.

Fig. 3 The point grid used for volume estimation. A point is infinitesimal and is defined as the intersection of the upper edge and the right edge of the lines in the upper right corner of each cross. The two magnocellular laminae are seen at the *lower left*. The counts for this field of view are: total LGN: five encircled points; parvocellular laminae: three encircled points; magnocellular laminae: 12 points; interlaminar regions: 19 points. Using the stereological software, the user indicates which region a point hits while the computer keeps track of the tallies

Estimation of neuron number using the optical fractionator

Independently, and subsequent to the above analysis of LGN volume, a second investigator (D.C.) reexamined the material to assess the number of neurons in the magnocellular and parvocellular parts of the LGN. For each section, the outline of the LGN was traced using a 4× objective (Olympus, UPlanApo, NA 0.16) at a final on-screen magnification of 105×. Each LGN was then divided into a magnocellular part and a parvocellular part by tracing between lamina 2 and 3, thereby splitting the interlaminar region, if present, into equal halves (Fig. 1c). The magnocellular and parvocellular laminae were usually

easily distinguished on the basis of their differences in cell size, with the magnocellular layer containing clearly larger cells. However, occasionally very small transitional regions were noted that contained cells with a gradual change in size. In these rare situations, the division was made in the middle such that cells mostly resembling magnocellular cells were included in the magnocellular part and vice versa. Finally, any magnocellular islands present were traced and included in the magnocellular part.

The sections were then examined using a $100\times$ oil immersion objective (Olympus, UPlanApo, NA 1.35) at a final onscreen magnification of $2,580\times$. One at a time, each of the two parts (magnocellular and parvocellular) were subsampled systematic uniformly random by $1,318 \mu m^2$ unbiased counting frames [37] in a square grid with a step-length of 140–350 μm (magnocellular) or 350–770 μm (parvocellular). The step-length was kept constant for all sections within the magnocellular or parvocellular part in a subject but adjusted to keep the number of sampled magno- as well as parvocellular neurons around 200 of each kind for each subject. For each subject, the step-length was chosen based upon the Cavalieri volume estimate for the respective magnocellular and parvocellular aminae of that brain and the mean magno- and parvocellular neuronal density of the LGN in the brains already analyzed. For the first brain, the density estimates were based upon pilot counts. This approach reduced the variability of the raw cell counts relative to the variation in total volume and neuron number across subjects, without compromising the

unbiased sampling scheme. Optical disector sampling in the z-axis was done with a disector height $h = 8 \mu m$ and an upper guard zone of 4.4 μm. The remaining (variable) thickness below the disector produced a lower guard zone that averaged 11.1 μm. The nucleolus of each neuron was used as the sampling unit; i.e., a neuron was counted if its nucleolus was sampled by an unbiased counting frame (Fig. 2a) and came into focus below the top, and above or at level with the bottom plane, of the disector. No neurons with more than one nucleolus were observed. Neurons were distinguished from astrocytes and oligodendrocytes by virtue of their clearly visible Nissl substance and proximal dendritic processes (Fig. 2). The 4.4 μm upper guard zone, which corresponds to $\sim 15 \mu m$ in the initial 80 μm thickness of the sections, was found optimal in a pilot calibration study of one LGN. In the calibration study, neuronal nucleoli were sampled systematic uniformly random for both the magno- and parvocellular parts of the LGN as described above, but without guard zones (i.e., in the full thickness of the section), and their z-positions recorded together with the respective local section thickness measured centrally in the counting frame. A uniform distribution of nucleoli was observed in the center of the section (Fig. 4, top row). However, near the top and bottom of the sections, corresponding to 5–10 μm in the initial 80-μm sections, fewer nucleoli were observed, indicating the effect of lost caps [4]. As a quality control, the z-positions of all nucleoli sampled across all 29 brains in the study were plotted. The resulting top hat plot (Fig. 4, middle of
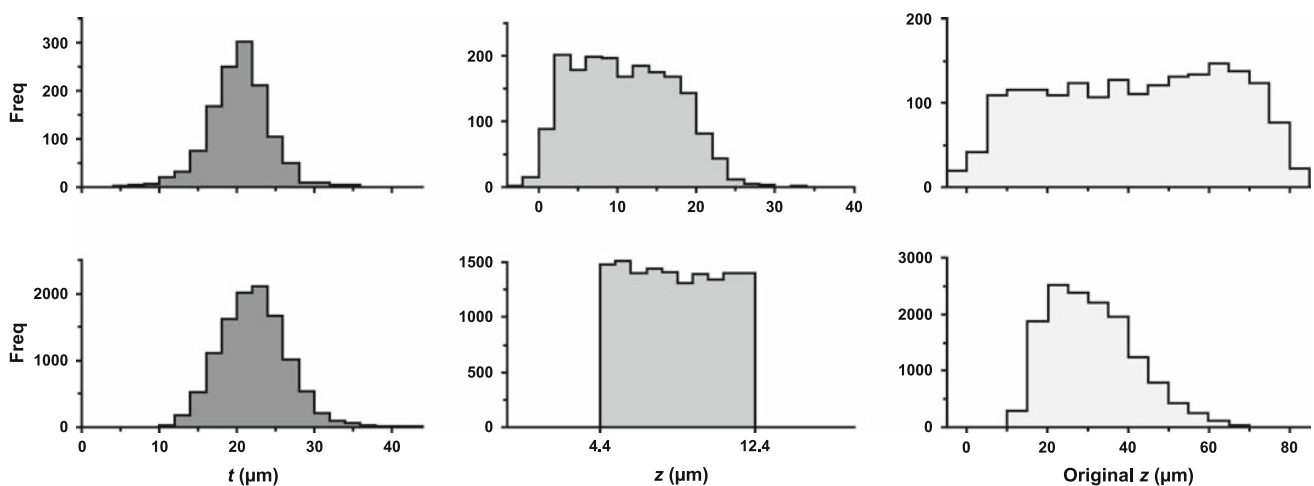
Fig. 4 *Top row* calibration study of left LGN in one subject that involved counting all neurons in the full section thickness. Section thickness was measured a total of 1,258 times and 1,869 neurons were counted across the magno- and parvocellular parts combined. *Bottom row* full study of the left LGN in all 29 subjects counting neurons in 8 μm high optical disectors with a top guard zone of 4.4 μm. A total of 11,256 section thicknesses were measured and 14,108 neurons counted across the magno- and parvocellular parts combined. *Left*

distribution of individual section thickness measurements. *Middle* position of neuronal nucleoli in the z-axis (i.e., distance from the top of section). R*ight* z-positions of neurons corrected for local shrinkage in the z-axis. Section thickness was measured in the center of each counting frame which also defined the local top and bottom of the section. Unevenness in the surfaces of the sections caused a few neurons to appear outside this range as seen in *top mid* and *left plots*

bottom row) corresponds to linear shrinkage in z-axis and verifies that we have a robust count despite the relatively low disector height of only 8 μm. The needed data for this kind of analysis are typically available when using a modern computerized stereology system, and we have routinely done this analysis in previous studies [29, 30, 50, 51].

The total numbers (N) of neurons in each of the two parts of the LGN were estimated using the fractionator method [38] as the product of the number of neuronal nucleoli counted in a known, uniformly random sample of the region of interest and the reciprocal sampling fraction. Using the optical fractionator [27, 81] this can be formulated as:

$$N := \frac{1}{\text{ssf}} \cdot \frac{1}{\text{asf}} \cdot \frac{\overline{t_{Q^-}}}{h} \cdot \sum Q^- \tag{2}$$

$$\overline{t_{Q^-}} = \frac{\sum (t_i \cdot q_i^-)}{\sum q_i^-} \tag{3}$$

where ssf is the section sampling fraction, asf the area sampling fraction, $\overline{t_{Q^-}}$ the number-weighted mean section thickness, $\sum Q^-$ the total number of neurons sampled by the optical disector probes of height h, and t_i the (final) local section thickness in the ith counting frame with a corresponding disector count of q_i^-. This version of the optical fractionator is robust to the pronounced and variable z-axis shrinkage observed in most cryostat or vibratome sections [27, 31]. We measured t_i centrally in every counting frame, where neurons were sampled, by focusing from the top to bottom of the section. In the present study, $1/\text{ssf} = 8$, $1/\text{asf} = 14.9$–92.9 for the magnocellular part and $1/\text{asf} = 92.9$–449.8 for the parvocellular part and $\overline{t_{Q^-}}/h \approx 2.72$ for the magnocellular part and $\overline{t_{Q^-}}/h \approx 2.97$ for the parvocellular part. The last value differed across subjects due to the variations in mean section thickness between subjects (magnocellular range: 16.5–26.5 μm, parvocellular range: 17.1–29.1 μm). The parvocellular mean section thickness (23.8 μm) was 9.5% greater than the magnocellular mean section thickness (21.7 μm).

An average of 651 (414–1,322) magnocellular counting frames and 422 (250–1,010) parvocellular counting frames were sampled per subject, and an average of 235 (133–499) magnocellular neurons and 252 (153–587) parvocellular neurons were counted per subject. The wide ranges in the number of frames and neurons sampled reflect that we aimed for a count of 400 neurons from each part of the LGN for the first four subjects. However, it was then clear that the counts could be halved without compromising the overall precision. Thus, for the last 25 subjects we obtained an average of 201 magnocellular and 210 parvocellular neurons.

Evaluation of the precision of the estimates

To assess the precision of the stereological estimates we determined the corresponding coefficients of error (CE) using the methods described by Gundersen et al. [39, 40]. We used the equations based on smoothness class $m = 1$ (in the terminology of Gundersen et al. [40]) for all cases where the LGN was contained in one thalamic block, as the areas and cell counts for the various compartments changed very smoothly from section to section despite the very irregular pattern within sections. For the 11 cases where the LGN spanned two thalamic blocs we used the model based upon smoothness class $m = 0$, because of the blunt start or end of blocks due to the split. This approach is conservative as some of the split LGNs appeared smooth for each block due to the incomplete sections at the transition between the blocks. For the 11 cases in which the left LGN was split into two blocks, the volumes and neuron numbers were estimated for each block and summed to give the total estimates. In these cases, the respective CEs were estimated for each block and then combined to give the CE_{total} of the combined estimates by:

$$\text{CE}_{\text{total}} = \frac{\sqrt{(\text{CE}_A \cdot \text{Est}_A)^2 + (\text{CE}_B \cdot \text{Est}_B)^2}}{(\text{Est}_A + \text{Est}_B)}, \tag{4}$$

where Est_A and Est_B are the relevant estimates from block A and B, and CE_A and CE_B are the respective CE estimates.

Our sampling scheme led to mean CEs of 0.02 to 0.04 for the volume estimates and 0.06 to 0.08 for the estimates of total neuron number (Table 2). These CEs are low compared to the observed variation across subjects, indicating that the scatter of our data predominantly reflects the real biological variability. Analysis of the subcomponents of the CEs indicated that the number of sections used per subject (9–16) was appropriate, and that sufficient numbers of points and neurons were counted.

The distinct outer boundaries of the LGN ensure precise delineation and estimation of the total volume and neuron number in contrast to other regions of the human brain where the recognition of subtle boundaries can impact the precision of stereological estimates [76]. However, as illustrated in Fig. 3, the exact boundaries between individual laminae are distinct but difficult and time consuming to trace in their full extent for the complete LGN. Consequently, we divided the current study into two parts. In Part One, the speed and ease of evaluating which region a point hit permitted us to assess the volume of all three compartments in a very efficient way (one to two brains a day) without the need of any time consuming tracing that could compromise the accuracy and precision of the estimates. In Part Two, we used tracing to subdivide the LGN along the

Table 2 Summary of the results of stereological analyses

		V_{tot} mm^3	CE	V_M mm^3	CE	V_P mm^3	CE	V_I mm^3	CE
Comparison	Mean	104	0.04	11.8	0.04	77.5	0.04	15.2	0.04
	CV	0.22		0.30		0.21		0.31	
Schizophrenia	Mean	111	0.03	12.2	0.04	84.2	0.04	16.4	0.04
	CV	0.16		0.21		0.14		0.31	
Mood disorders	Mean	126	0.02	13.6	0.03	91.7	0.03	21.4	0.02
	CV	0.11		0.19		0.09		0.23	
		N_{tot} (10^6)	CE	N_M (10^6)	CE	N_P (10^6)	CE		
Comparison	Mean	1.77	0.07	0.223	0.08	1.55	0.07		
	CV	0.20		0.24		0.20			
Schizophrenia	Mean	2.02	0.06	0.249	0.08	1.77	0.07		
	CV	0.27		0.32		0.27			
Mood disorders	Mean	2.08	0.06	0.251	0.08	1.83	0.07		
	CV	0.17		0.22		0.18			

V_{tot} is the estimated total volume of the left LGN; V_M, V_P, and V_I, the volumes of the magnocellular and parvocellular laminae as well as the interlaminar regions, respectively. N_{tot} the estimated total number of neurons in the left LGN. N_M and N_P the estimated numbers of neurons in the magnocellular and parvocellular parts of the LGN, respectively. Mean estimator coefficient of error (CE) and inter-individual coefficient of variation (CV) are listed for all measures. The mean CEs are calculated for each group as the square root of the mean of the respective squared CE estimates for each individual within the group

very clear boundary between the magno- and parvocellular parts, and estimated the neuron number within each part. Because of the distinct nature of the boundary between magno- and parvocellular regions, both regions were well-defined and the neuron number estimates were robust. Tracing all the individual laminae as a basis for volume and neuron number estimation would be very time consuming and would lead to less precise and potentially biased estimates as the reference space itself would be less well-defined.

Statistical methods

To compare the volumes and neuron numbers of the LGN and its constituent compartments among subjects with schizophrenia, subjects with mood disorders and control subjects, analysis of covariance (ANCOVA) models were used with diagnosis as the main effect and sex, age, PMI and storage time as covariates. A secondary ANCOVA analysis examined the effect of brain weight in addition to the previously noted covariates. No significant differences between the two models were found in term of the conclusions, with the only noticeable difference being the subtle change in significance level for diagnostic effect for parvocellular volume ($P = 0.049$ without brain weight, and $P = 0.068$ with brain weight). Post hoc testing of pairwise differences between diagnostic groups was also

conducted. Due to the relatively small sample sizes, no adjustments for multiple comparisons were made to the P values for these pairwise comparisons. These analyses were implemented in SAS PROC GLM [55].

Fisher's z transformation was used to test Pearson correlation coefficients between LGN volumes estimated by the two methods, as well as the correlations between neuron number and total volume for the LGN for all subjects and also by diagnostic group. Analyses were implemented in SAS PROC CORR.

All statistical tests were two-sided and conducted with an alpha level = 0.05.

Production details for micrographs

All micrographs for Figs. 1, 2 and 3 were obtained using a Zeiss AxioCam digital camera on a Zeiss Axiophot microscope. Figure 1 is an x-, y-axes montage obtained with a 2.5× (Zeiss, Plan Neofluar, NA .075) objective, Fig. 2a, b are z-axis montages obtained with a 100× (Zeiss, Plan Neofluar, NA 1.30) objective, and Fig. 3 was obtained with a 5× (Zeiss, Plan Neofluar, NA 0.15) objective. The raw pictures of 3,900 × 3,090 pixels, 32-bit colors, were saved in tiff format using the camera software (AxioVision v. 3.1). Using Adobe PhotoShop, the multiple micrographs were cropped, adjusted for color balance, brightness, and contrast, and positioned into the montages (Figs. 1, 2 or 3).
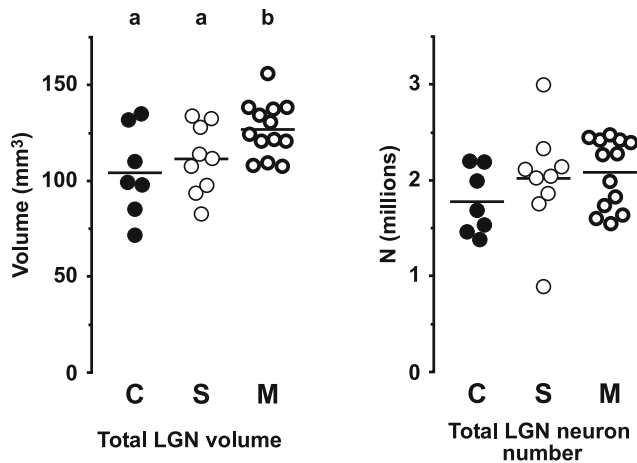
Fig. 5 Estimated total volume (*left*) and neuron number (*right*) of the left LGN for the comparison (*C*), schizophrenia (*S*), and mood disorders (*M*) groups of subjects. The *horizontal bars* indicate group means. *Lettering* at the top indicates significance. Groups not sharing the same letter are significantly different at $P < 0.05$

Results

The results of the study are summarized in Figs. 5, 6, 7, 8 and 9 and Table 2. As shown in Fig. 5 and Table 2, the three diagnostic groups differed significantly in left LGN mean volume ($F_{2,22} = 4.16$, $P = 0.029$). Calculated from the raw estimates, this difference was due to a 21.6% greater mean left LGN volume in the subjects with mood disorders (M) relative to the comparison subjects (C); the subjects with schizophrenia (S) showed a 6.8% greater volume. In contrast no significant differences were detected among the groups in total neuron number (S vs. C: +13.8%, M vs. C: +17.4%, $F_{2,22} = 0.82$, $P = 0.45$). As shown in Fig. 6, the volume differences were driven partly by the interlaminar regions, where a marked and significant increase in mean volume in the mood disorder group was evident (S vs. C: +7.7%, M vs. C: +40.7%, $F_{2,22} = 4.22$, $P = 0.028$), and partly by the parvocellular aminae, that
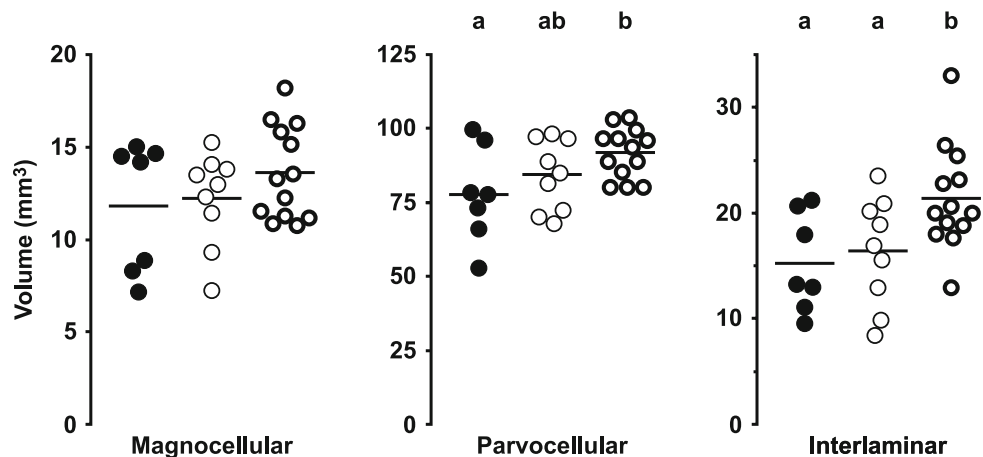
also showed a significant increase in mean volume (S vs. C: +8.6%, M vs. C: +18.3%, $F_{2,22} = 3.48$, $P = 0.049$). In contrast, no significant differences in mean volume of the magnocellular laminae were present (S vs. C: +3.5%, M vs. C: +15.2%, $F_{2,22} = 1.30$, $P = 0.29$). As indicated in Fig. 7, no significant differences in mean neuron number were observed across the three diagnostic groups in either the magnocellular part (S vs. C: +11.4%, M vs. C: +12.6%, $F_{2,22} = 0.28$, $P = 0.76$) or the parvocellular part (S vs. C: +14.2%, M vs. C: +18.1%, $F_{2,22} = 0.90$, $P = 0.42$). As shown in Fig. 8, we observed a strong correlation between total volume and total neuron number across all subjects ($r = 0.64$, $P = 0.0002$). Finally, as illustrated in Fig. 9, the two investigators showed high agreement in their independent identifications of the LGN. Estimates of total LGN volume via Cavalieri's principle based upon point counting (as reported in Fig. 5, left) strongly corresponded with those based upon the areas of the traces used for the cell counting ($r = 0.97$, $P < 0.0001$). As expected, tracing shows a small positive bias of 4.9% compared to the point counts, the latter being methodologically unbiased (bias calculated as the difference between mean tracing based volume and mean point count based volume relative to the latter of these). However, as the added extra volume is very minor and involves the cell sparse white matter surrounding the LGN, this difference does not compromise the neuron number estimates. In all analysis, no significant effects were seen for any of the covariates (sex, age, PMI, tissue storage time).

Correlation plots for the volume and total neuron number of the left LGN versus the left BA17 for the eight subjects included both here and in our previous BA17 study [30] are shown in Fig. 10. A strong positive correlation ($r = 0.982$, $P = 0.0005$) between LGN and BA17 volume were observed for the schizophrenia group. Also, a positive correlation ($r = 0.891$, $P = 0.017$) was present between the neuron numbers of LGN and BA17. However, the latter correlation should be interpreted with care as it is driven by

Fig. 6 Estimated volumes of the three compartments of the left LGN for the comparison (*filled circles*), schizophrenia (*thin circles*), and mood disorders (*bold circles*) groups of subjects. The *horizontal bars* indicate group means. *Lettering* at the top indicates significance. Groups not sharing the same letter are significantly different at $P < 0.05$
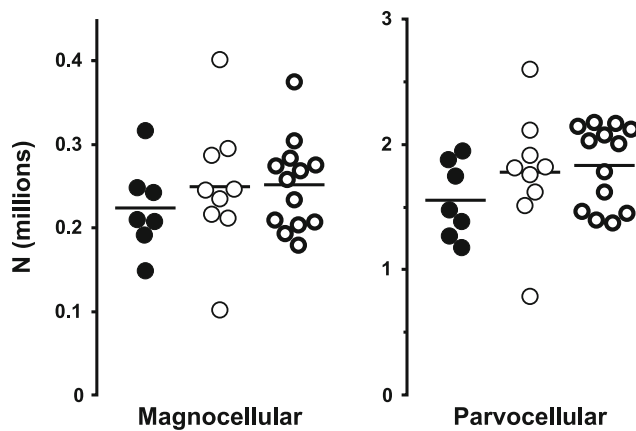
Fig. 7 Estimated neuron numbers of the two parts of the left LGN for the comparison (*filled circles*), schizophrenia (*thin circles*), and mood disorders (*bold circles*) groups of subjects. The *horizontal bars* indicate group means
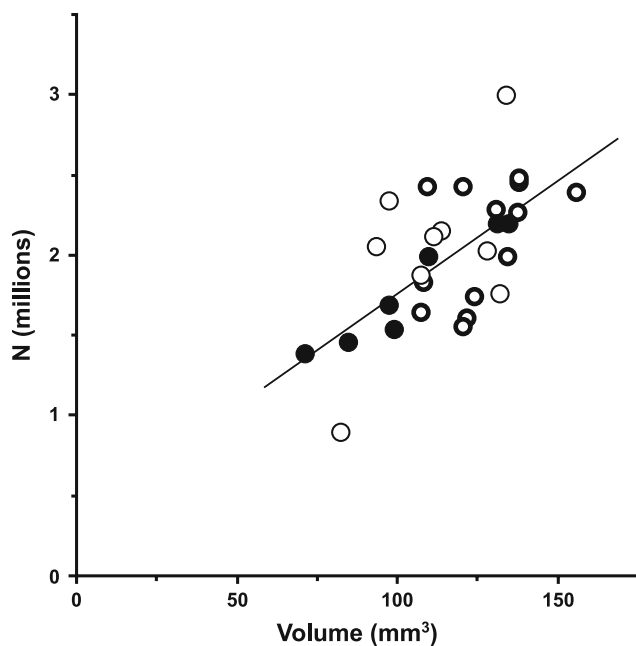
Fig. 8 Scatterplot demonstrating the positive correlation ($r = 0.64$, $P = 0.0002$) between total neuron number and volume of LGN. *Filled circles* indicate subjects from the comparison group, *thin circles* represent subjects from the schizophrenia group, and *bold circles* symbolize subjects from the mood disorder group. *Line* is the regression line

a single subject in the lower left of the plot. As only two control subjects are shared between the two studies, it is not meaningful to perform correlations for that group.

Discussion

The present study did not reveal any significant differences in volume or neuron number of the compartments of the LGN in subjects with schizophrenia relative to the normal comparison subjects. Unexpectedly, we did observe that the subjects with mood disorders had a greater volume of the interlaminar regions (+41%) and the parvocellular laminae (+18%) relative to the normal comparison subjects.

Limitations of the current study

Like many postmortem studies, the current study is limited by the relative small number of subjects. In addition, our schizophrenia group is diagnostically heterogeneous with three subjects diagnosed with schizoaffective disorder and three subjects with a history of alcohol or other substance disorder. Therefore, we included a second comparison group of subjects with mood disorders, many of whom had a history of alcohol or other substance disorder, to test the specificity of any finding in the schizophrenia group. Unfortunately, the resulting very heterogeneous nature of this third group of subjects prevents us from drawing robust conclusions from the unexpected findings of increased volume of the left LGN, the parvocellular lamina and especially the interlaminar regions in these subjects. It may be noted that the variability of the three subject groups are comparable for the main result variables as seen in Table 2 and Figs. 5, 6 and 7. The diagnostic heterogeneities within the schizophrenia group and the mood group do therefore not appear to inflate the variance of the assessed parameters.

In addition, all the subjects in the schizophrenia group and three of the subjects in the mood disorder group had received antipsychotic therapy. However, in our previous study of the MD [29], we evaluated a cohort of nonhuman primates that had been exposed to antipsychotics and did not see any medication-related differences in the MD. Also, in a postmortem study of the MD, Pakkenberg observed similar volume reductions in two schizophrenia groups of subjects treated and untreated with antipsychotics, respectively [60]. It is therefore unlikely that antipsychotic medication had any impact on our findings.

Also, it should be pointed out that although we used methods based upon unbiased principles, all volume estimates using histological tissue samples will be biased due to the shrinkage during the processing. It is known that the initial fixation and cryoprotection introduces marked tissue shrinkage with variations from subject to subject and from brain region to brain region—see e.g., [28]. It is unknown whether such biases are constant across diagnosis groups; indeed, a recent study of the hippocampus reported a significant 18% greater shrinkage in the z-axis of sections from subjects with major depression relative to control subjects [73]. In the current study, we observed a similar degree of mean z-shrinkage across all three subject groups. However, although unlikely, we cannot rule out differential shrinkage of our tissue prior to sectioning. In contrast, our
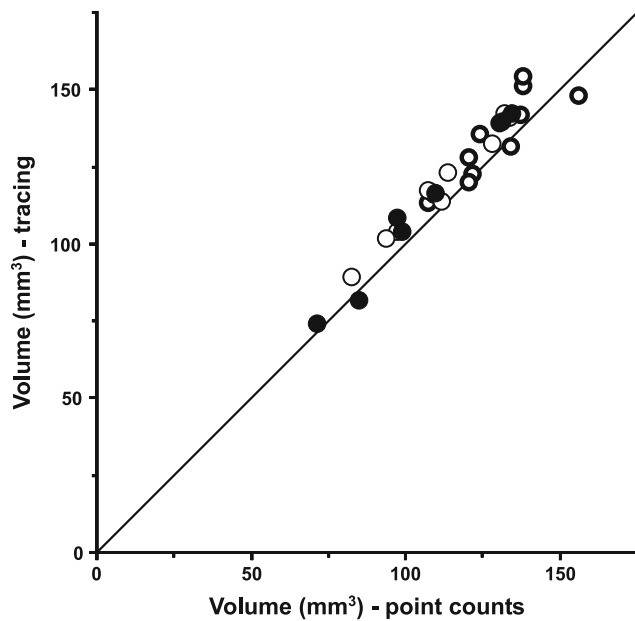
Fig. 9 Total volumes of the left LGN estimated by Cavalieri's principle from point counts (by RS) or tracing (by DC) for each subject from the comparison (*filled circles*), schizophrenia (*thin circles*), and mood disorders (*bold circles*) groups. *Line* is the identity line

estimates of neuron numbers are not biased by tissue shrinkage.

Comparison with previous studies

The main findings of our study, the absence of schizophrenia-related changes in the total volume and neuron number of the magnocelluar and parvocellular laminae of the LGN,

are in agreement with the two previous postmortem studies of the LGN in schizophrenia [54, 64]. Surprisingly, the latter study, which is based upon stereological methods comparable to our study, reports a 75% higher estimated number of total LGN neurons (132% higher magno- and 67% higher parvocellular numbers) than our findings. In Table 3 we list previous estimates of neuron number in the human LGN; our mean total neuron number agrees more closely with the numbers reported by older studies than do the numbers reported by Selemon and Begović. However, as only the study by Selemon and Begović and our own study use methods based upon unbiased stereological principles, the comparison to the other studies cited in Table 3 should be interpreted with great care.

The reasons for the discrepancy in total neuron number between our study and the study by Selemon and Begović are unclear: (1) it is unlikely that differences in the subject samples are the reason as close inspection does not reveal any obvious differences in subject demographics between the two studies that are likely to explain the observed difference in neuron number. (2) Differences in delineation of the LGN are unlikely because of the distinct borders of the nucleus, and because the volume estimates are reasonably similar for the two studies when taking differences in processing into account. (3) It should be noted that Selemon and Begović report only cell counts from the magno- and parvocellular laminae while we included neurons from the cell sparse interlaminar regions. This would increase our estimates compared to those of Selemon and Begović's, and thus cannot explain the difference in findings. (4) It is also unlikely that investigator differences in the classification of cells as neurons or glia
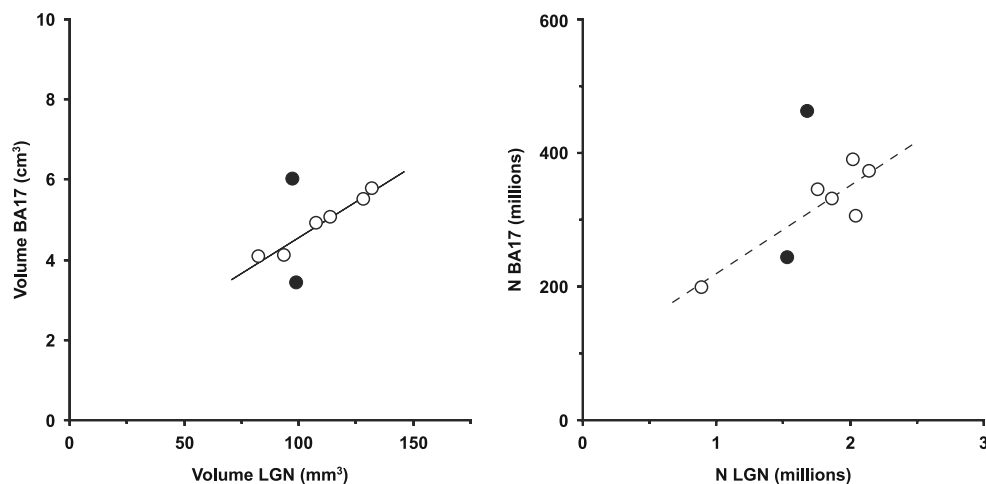
Fig. 10 Correlation plots for volume and total neuron number of the left LGN versus the left BA17 for the eight subjects included in both this study and our previous study of BA17 [30]. *Filled circles* indicate comparison subjects and *open circles* indicate subjects with schizophrenia. *Lines* are correlation lines for the schizophrenia group

($r = 0.982$, $P = 0.0005$, and $r = 0.891$, $P = 0.017$, *left* and *right* plot, respectively). The *broken correlation line* at right indicates that the correlation should be interpreted with care as it is predominantly due to the single subject in the lower left of the plot

Table 3 Findings of previous studies of the number of neurons in the human LGN

Study	n	N_{tot}	N_M	N_P
Balado and Franke, 1937 [10]	1	568,845	86,181	482,664
Chacko, 1948 [21]	1	1,210,000	111,000	1,099,000
Sullivan et al., 1958 [74]	1	1,018,190		
Kupfer et al., 1967 [52]	1	1,043,000	62,500	980,500
Armstrong, 1979 [9]	2	2,172,000		
Khan et al., 1993 [49]	2	1,680,000		
Selemon and Begović, 2007 [64]	30	3,476,698	565,835	2,910,863
Current study	29	1,990,000	244,000	1,740,000

n is number of subjects, while N_{tot}, N_M, and N_P the estimated mean neuron numbers of the whole LGN, the magnocellular region, and parvocellular region, respectively. The study by Khan et al. was based upon brains from two late gestational fetuses (gestational age of 34–35 weeks). For the last two studies the values represent all subjects across all diagnostic groups as neither study found significant group differences. Only the last two studies were based upon unbiased stereological techniques

are the reason: When the current material was examined in our previous study of the MD, we were able to consistently identify a class of small thalamic neurons, leading to higher neuron numbers than estimated in other studies [29]. Recently, several stereological studies have reported neuron numbers for the MD comparable to ours [1, 59, and Pakkenberg, personal communication]. The Stanley Foundation material [77] used by Selemon and Begović has also previously been used in a study of the MD [82], which like our previous study did not find a schizophrenia-related difference in MD neuron number. However, Young et al. estimated markedly fewer neurons in the MD than we did. It is therefore unlikely that differences in ability to recognize neurons in the current study would lead us to count markedly fewer neurons than Selemon and Begović.

In the end, handling of the section thickness seems to be the only clear difference between the two studies. Thus, in the current study we used methods robust to the marked shrinkage in the z-axis seen in cryostat sections [27]. Especially, we measured the section thickness in every counting frame where neurons were sampled. This strategy is particular important as we observed a systematic difference in section thickness between the magnocellular and parvocellular parts of the LGN (P vs. M: +9.5%, paired t test: $t_{28} = 11.3$, $P < 0.0001$). In contrast, it is not clear from the paper of Selemon and Begović how they assessed section thickness. Due to the unusual processing of their tissue (paraffin embedding with subsequent deparaffination, cryoprotection and cryostat sectioning), they had a very marked z-collapse and were only able to use an optical disector of very limited height (6 μm). It is therefore unclear if, their determination of the section thickness sampling fraction may have been compromised. Also,

incidences of nonlinear z-collapse biasing the use of the optical disector or fractionator have been reported [11, 34]. We have not observed this effect in either the current study or in any of our previous studies, but have always checked for it as part of our calibration study for determination of guard zone size (Fig. 4). Selemon and Begović did not report performing such a calibration study.

Relation to our previous findings of a reduced BA17 in schizophrenia

The ingrowth of afferents from the thalamus during prenatal development has been shown to determine the area and volume of cytoarchitectonic regions in the cerebral cortex [67, 75, 80]. In particular, it has been demonstrated in monkeys that developmentally reducing the volume of the LGN by intrauterine enucleation [25, 62] or thalamic irradiation [2, 63, 65] leads to a smaller volume of BA17.

Unfortunately, only two comparison and six schizophrenia subjects from the current study were also included in our previous study of the primary visual cortex [30]. Thus, the archival material used in the current study precludes performing a rigorous regression analysis of findings in LGN and BA17. Consequently, we cannot directly test the hypothesis that the previously observed reduction in BA17 volume and total neuron number in schizophrenia reflects a smaller set of inputs from the LGN, although the results of the present and the two previous studies [54, 64] do not support this interpretation. Interestingly, we observed a strong and significant correlation between the LGN and BA17 volume estimates for the six subjects in the schizophrenia group. This observation agrees with previous findings in normal subjects [6]—see also [22]. With corresponding LGN and BA17 data from only two comparison subjects we are not able to determine if the LGN-BA17 regression line of the subjects with schizophrenia is shifted, has a different slope or both compared to the relation in comparison subjects.

All in all, the current study as well as the two previous studies of the LGN [54, 64] do not provide evidence for the LGN as a primary disturbance driving our previous BA17 findings. Consequently, to the extent that the latter observations are common in schizophrenia, they are likely to reflect another process. Interestingly, it has been demonstrated that intracortical gradients of various growth factors and receptors such as FGF8 and EphA also are important for determining the area and volume of cytoarchitectonic regions in the cerebral cortex [33, 61, 66, 68]. It is therefore possible that changes in such intracortical developmental factors account for the previously observed reduction of BA17 in schizophrenia.

Furthermore, we did not see specific changes in the magnocellular or parvocellular laminae of the LGN. Therefore, our data do not provide additional insight into

the magnocellular pathway/dorsal stream specific impairment of the visual system in subjects with schizophrenia described in the literature [15, 16, 23, 48, 53].

Interestingly, while LGN "upstream" to BA17 does not show structural changes in schizophrenia, at least one structure "downstream" of BA17 shows robust changes: The pulvinar is an association nucleus of the thalamus involved in higher-order visual processing, and receives direct input from BA17 [36, 69]. A substantial number of postmortem studies have reported smaller pulvinar volume and neuron number in schizophrenia [12, 18, 19, 24, 43, 54]—although the pulvinar volume reductions of the first two studies [12, 54] did not reach significance. Also, smaller pulvinar volume in schizophrenia has been reported by several imaging studies [17, 35, 47]. Thus, robust structural changes in the visual system in schizophrenia may be downstream to the LGN.

Conclusion

The findings of the current study do not support the hypothesis that subjects with schizophrenia have structural changes in the LGN. Therefore, our previous observation of a schizophrenia-related reduction of the primary visual cortex is probably not caused by a reduction in LGN. However, further studies are warranted to elucidate precisely the correlational relations between size of LGN versus BA17 in subjects with and without schizophrenia. Also, our unexpected finding of an increased volume of the LGN in subjects with mood disorders requires replication due to the heterogeneous nature of the group and the serendipitous character of the finding.

References

1. Abitz M, Nielsen RD, Jones EG, Laursen H, Graem N, Pakkenberg B (2007) Excess of neurons in the human newborn mediodorsal thalamus compared with that of the adult. Cereb Cortex 17:2573–2578. doi:10.1093/cercor/bhl163

2. Algan O, Rakic P (1997) Radiation-induced, lamina-specific deletion of neurons in the primate visual cortex. J Comp Neurol 381:335–352. doi:10.1002/(SICI)1096-9861(19970512)381:3<335::AID-CNE6>3.0.CO;2-3

3. American Psychiatric Association (1994) DSM-IV. Diagnostic and statistical manual of mental disorders, 4th edn. American Psychiatric Association, Washington, DC

4. Andersen BB, Gundersen HJG (1999) Pronounced loss of cell nuclei and anisotropic deformation of thick sections. J Microsc 196:69–73. doi:10.1046/j.1365-2818.1999.00555.x

5. Andreasen NC, O'Leary DS, Flaum M, Nopoulos P, Watkins GL, Boles Ponto LL et al (1997) Hypofrontality in schizophrenia: distributed dysfunctional circuits in neuroleptic-naïve patients. Lancet 349:1730–1734. doi:10.1016/S0140-6736(96)08258-X

6. Andrews TJ, Halpern SD, Purves D (1997) Correlated size variations in human visual cortex, lateral geniculate nucleus, and optic tract. J Neurosci 17:2859–2868

7. Ardekani BA, Bappal A, D'Angelo D, Ashtari M, Lencz T, Szeszko PR et al (2005) Brain morphometry using diffusion-weighted magnetic resonance imaging: application to schizophrenia. NeuroReport 16:1455–1459. doi:10.1097/01.wnr.0000177001.27569.06

8. Ardekani BA, Nierenberg J, Hoptman MJ, Javitt DC, Lim KO (2003) MRI study of white matter diffusion anisotropy in schizophrenia. NeuroReport 14:2025–2029. doi:10.1097/00001756-200311140-00004

9. Armstrong E (1979) A quantitative comparison of the hominoid thalamus. I. Specific sensory relay nuclei. Am J Phys Anthropol 51:365–382. doi:10.1002/ajpa.1330510308

10. Balado M, Franke E (1937) Das Corpus geniculatum externum. In: Foerster O, Rüdin E, Spatz H (eds) Monog. a. d. Gesamtgeb. d. Neurol. u. Psychiat, vol 62, pp 1–118. Springer, Berlin

11. Baryshnikova LM, von Bohlen und Halbach O, Kaplan S, von Bartheld CS (2006) Two distinct events, section compression and loss of particles ("lost caps"), contribute to z-axis distortion and bias in optical disector counting. Microsc Res Tech 69:738–756. doi:10.1002/jemt.20345

12. Bogerts B, Falkai P, Haupts M, Greve B, Ernst S, Tapernon-Franz U et al (1990) Post-mortem volume measurements of limbic system and basal ganglia structures in chronic schizophrenics. Initial results from a new brain collection. Schizophr Res 3:295–301. doi:10.1016/0920-9964(90)90013-W

13. Butler PD, Hoptman MJ, Nierenberg J, Foxe JJ, Javitt DC, Lim KO (2006) Visual white matter integrity in schizophrenia. Am J Psychiatry 163:2011–2013. doi:10.1176/appi.ajp.163.11.2011

14. Butler PD, Javitt DC (2005) Early-stage visual processing deficits in schizophrenia. Curr Opin Psychiatry 18:151–157. doi:10.1097/00001504-200503000-00008

15. Butler PD, Martinez A, Foxe JJ, Kim D, Zemon V, Silipo G et al (2007) Subcortical visual dysfunction in schizophrenia drives secondary cortical impairments. Brain 130:417–430. doi:10.1093/brain/awl233

16. Butler PD, Zemon V, Schechter I, Saperstein AM, Hoptman MJ, Lim KO et al (2005) Early-stage visual processing and cortical amplification deficits in schizophrenia. Arch Gen Psychiatry 62:495–504. doi:10.1001/archpsyc.62.5.495

17. Byne W, Buchsbaum MS, Kemether E, Hazlett EA, Shinwari A, Mitropoulou V et al (2001) Magnetic resonance imaging of the thalamic mediodorsal nucleus and pulvinar in schizophrenia and schizotypal personality disorder. Arch Gen Psychiatry 58:133–140. doi:10.1001/archpsyc.58.2.133

18. Byne W, Buchsbaum MS, Mattiace LA, Hazlett EA, Kemether E, Elhakem SL et al (2002) Postmortem assessment of thalamic nuclear volumes in subjects with schizophrenia. Am J Psychiatry 159:59–65. doi:10.1176/appi.ajp.159.1.59

19. Byne W, Fernandes J, Haroutunian V, Huacon D, Kidkardnee S, Kim J et al (2007) Reduction of right medial pulvinar volume and neuron number in schizophrenia. Schizophr Res 90:71–75. doi:10.1016/j.schres.2006.10.006

20. Callaway EM (2005) Structure and function of parallel pathways in the primate early visual system. J Physiol 566:13–19. doi:10.1113/jphysiol.2005.088047

21. Chacko LW (1948) The laminar pattern of the lateral geniculate body in the primates. J Neurol Neurosurg Psychiatry 11:211–224

22. Chen W, Zhu X-H (2001) Correlation of activation sizes between lateral geniculate nucleus and primary visual cortex in humans. Magn Reson Med 45:202–205. doi:10.1002/1522-2594(200102)45:2<202::AID-MRM1027>3.0.CO;2-S

23. Chen Y, Levy DL, Sheremata S, Holzman PS (2004) Compromised late-stage motion processing in schizophrenia. Biol Psychiatry 55:834–841. doi:10.1016/j.biopsych.2003.12.024

24. Danos P, Baumann B, Krämer A, Bernstein H-G, Stauch R, Krell D et al (2003) Volumes of association thalamic nuclei in schizophrenia: a postmortem study. Schizophr Res 60:141–155. doi:10.1016/S0920-9964(02)00307-9

25. Dehay C, Giroud P, Berland M, Killackey H, Kennedy H (1996) Contribution of thalamic input to the specification of cytoarchitectonic cortical fields in the primate: effects of bilateral enucleation in the fetal monkey on the boundaries, dimensions, and gyrification of striate and extrastriate cortex. J Comp Neurol 367:70–89. doi:10.1002/(SICI)1096-9861(19960325)367:1<70::AID-CNE6>3.0.CO;2-G

26. Desco M, Gispert JD, Reig S, Sanz J, Pascau J, Sarramea F et al (2003) Cerebral metabolic patterns in chronic and recent-onset schizophrenia. Psychiatry Res 122:125–135. doi:10.1016/S0925-4927(02)00124-5

27. Dorph-Petersen K-A, Nyengaard JR, Gundersen HJG (2001) Tissue shrinkage and unbiased stereological estimation of particle number and size. J Microsc 204:232–246. doi:10.1046/j.1365-2818.2001.00958.x

28. Dorph-Petersen K-A, Pierri JN, Perel JM, Sun Z, Sampson AR, Lewis DA (2005) The influence of chronic exposure to antipsychotic medications on brain size before and after tissue fixation: a comparison of haloperidol and olanzapine in macaque monkeys. Neuropsychopharmacology 30:1649–1661. doi:10.1038/sj.npp.1300710

29. Dorph-Petersen K-A, Pierri JN, Sun Z, Sampson AR, Lewis DA (2004) Stereological analysis of the mediodorsal thalamic nucleus in schizophrenia: volume, neuron number, and cell types. J Comp Neurol 472:449–462. doi:10.1002/cne.20055

30. Dorph-Petersen K-A, Pierri JN, Wu Q, Sampson AR, Lewis DA (2007) Primary visual cortex volume and total neuron number are reduced in schizophrenia. J Comp Neurol 501:290–301. doi:10.1002/cne.21243

31. Dorph-Petersen K-A, Rosenberg R, Nyengaard JR (2004) Estimation of number and volume of immunohistochemically stained neurons in complex brain regions. In: Evans SM, Janson AM, Nyengaard JR (eds) Quantitative methods in neuroscience. A neuroanatomical approach. Oxford University Press, Oxford, pp 216–240

32. Fowler IL, Carr VJ, Carter NT, Lewin TJ (1998) Patterns of current and lifetime substance use in schizophrenia. Schizophr Bull 24:443–455

33. Fukuchi-Shimogori T, Grove EA (2001) Neocortex patterning by the secreted signaling molecule FGF8. Science 294:1071–1074. doi:10.1126/science.1064252

34. Gardella D, Hatton WJ, Rind HB, Rosen GD, von Bartheld CS (2003) Differential tissue shrinkage and compression in the z-axis: implications for optical disector counting in vibratome-, plastic- and cryosections. J Neurosci Methods 124:45–59. doi:10.1016/S0165-0270(02)00363-1

35. Gilbert AR, Rosenberg DR, Harenski K, Spencer S, Sweeney JA, Keshavan MS (2001) Thalamic volumes in patients with first-episode schizophrenia. Am J Psychiatry 158:618–624. doi:10.1176/appi.ajp.158.4.618

36. Grieve KL, Acuña C, Cudeiro J (2000) The primate pulvinar nuclei: vision and action. Trends Neurosci 23:35–39. doi:10.1016/S0166-2236(99)01482-4

37. Gundersen HJG (1977) Notes on the estimation of the numerical density of arbitrary profiles: the edge effect. J Microsc 111:219–223

38. Gundersen HJG (1986) Stereology of arbitrary particles. A review of unbiased number and size estimators and the presentation of some new ones, in memory of William R. Thompson. J Microsc 143:3–45

39. Gundersen HJG, Jensen EB (1987) The efficiency of systematic sampling in stereology and its prediction. J Microsc 147:229–263

40. Gundersen HJG, Jensen EBV, Kiêu K, Nielsen J (1999) The efficiency of systematic sampling in stereology—reconsidered. J Microsc 193:199–211. doi:10.1046/j.1365-2818.1999.00457.x

41. Hendry SHC, Reid RC (2000) The koniocellular pathway in primate vision. Annu Rev Neurosci 23:127–153. doi:10.1146/annurev.neuro.23.1.127

42. Hickey TL, Guillery RW (1979) Variability of laminar patterns in the human lateral geniculate nucleus. J Comp Neurol 183:221–246. doi:10.1002/cne.901830202

43. Highley JR, Walker MA, Crow TJ, Esiri MM, Harrison PJ (2003) Low medial and lateral right pulvinar volumes in schizophrenia: a postmortem study. Am J Psychiatry 160:1177–1179. doi:10.1176/appi.ajp.160.6.1177

44. Hirai T, Jones EG (1989) A new parcellation of the human thalamus on the basis of histochemical staining. Brain Res Brain Res Rev 14:1–34. doi:10.1016/0165-0173(89)90007-6

45. Howard CV, Reed MG (1998) Unbiased stereology. Three-dimensional measurement in microscopy. Bios Scientific Publishers, Oxford

46. Jones EG (2007) The lateral geniculate nucleus. In: Jones EG (ed) The thalamus, 2nd edn. Cambridge University Press, Cambridge, pp 924–1008

47. Kemether EM, Buchsbaum MS, Byne W, Hazlett EA, Haznedar M, Brickman AM et al (2003) Magnetic resonance imaging of mediodorsal, pulvinar, and centromedian nuclei of the thalamus in patients with schizophrenia. Arch Gen Psychiatry 60:983–991. doi:10.1001/archpsyc.60.9.983

48. Kéri S, Kiss I, Kelemen O, Benedek G, Janka Z (2005) Anomalous visual experiences, negative symptoms, perceptual organization and the magnocellular pathway in schizophrenia: a shared construct? Psychol Med 35:1445–1455. doi:10.1017/S0033291705005398

49. Khan AA, Wadhwa S, Pandey RM, Bijlani V (1993) Prenatal human lateral geniculate nucleus: a quantitative light microscopic study. Dev Neurosci 15:403–409. doi:10.1159/000111364

50. Konopaske GT, Dorph-Petersen K-A, Pierri JN, Wu Q, Sampson AR, Lewis DA (2007) Effect of chronic exposure to antipsychotic medication on cell numbers in the parietal cortex of macaque monkeys. Neuropsychopharmacology 32:1216–1223. doi:10.1038/sj.npp.1301233

51. Konopaske GT, Dorph-Petersen K-A, Sweet RA, Pierri JN, Zhang W, Sampson AR et al (2008) Effect of chronic antipsychotic exposure on astrocyte and oligodendrocyte numbers in macaque monkeys. Biol Psychiatry 63:759–765. doi:10.1016/j.biopsych.2007.08.018

52. Kupfer C, Chumbley L, Downer J DE C (1967) Quantitative histology of optic nerve, optic tract and lateral geniculate nucleus of man. J Anat 101:393–401

53. Laycock R, Crewther SG, Crewther DP (2007) A role for the 'magnocellular advantage' in visual impairments in

neurodevelopmental and psychiatric disorders. Neurosci Biobehav Rev 31:363–376. doi:10.1016/j.neubiorev.2006.10.003

54. Lesch A, Bogerts B (1984) The diencephalon in schizophrenia: evidence for reduced thickness of the periventricular grey matter. Eur Arch Psychiatry Neurol Sci 234:212–219. doi:10.1007/BF00381351

55. Littell RC, Stroup WW, Freund RJ (2002) SAS for linear models. Wiley-SAS, Hoboken

56. Livingstone M, Hubel D (1988) Segregation of form, color, movement, and depth: anatomy, physiology, and perception. Science 240:740–749. doi:10.1126/science.3283936

57. Livingstone MS, Hubel DH (1987) Psychophysical evidence for separate channels for the perception of form, color, movement, and depth. J Neurosci 7:3416–3468

58. Mishkin M, Ungerleider LG, Macko KA (1983) Object vision and spatial vision: two cortical pathways. Trends Neurosci 6:414–417. doi:10.1016/0166-2236(83)90190-X

59. Nielsen RD, Abitz M, Andersen BB, Pakkenberg B (2004) Neuron and glial cell numbers in subdivisions of the mediodorsal (MD) nucleus of the thalamus in schizophrenic subjects and controls. 2004 Abstract Viewer/Itinerary Planner. Society for Neuroscience, Washington, DC. Online. Program No. 110.7

60. Pakkenberg B (1992) The volume of the mediodorsal thalamic nucleus in treated and untreated schizophrenics. Schizophr Res 7:95–100. doi:10.1016/0920-9964(92)90038-7

61. Ragsdale CW, Grove EA (2001) Patterning the mammalian cerebral cortex. Curr Opin Neurobiol 11:50–58. doi:10.1016/S0959-4388(00)00173-2

62. Rakic P (1988) Specification of cerebral cortical areas. Science 241:170–176. doi:10.1126/science.3291116

63. Schindler MK, Wang L, Selemon LD, Goldman-Rakic PS, Rakic P, Csernansky JG (2002) Abnormalities of thalamic volume and shape detected in fetally irradiated rhesus monkeys with high dimensional brain mapping. Biol Psychiatry 51:827–837. doi:10.1016/S0006-3223(01)01341-5

64. Selemon LD, Begović A (2007) Stereologic analysis of the lateral geniculate nucleus of the thalamus in normal and schizophrenic subjects. Psychiatry Res 151:1–10. doi:10.1016/j.psychres.2006.11.003

65. Selemon LD, Wang L, Nebel MB, Csernansky JG, Goldman-Rakic PS, Rakic P (2005) Direct and indirect effects of fetal irradiation on cortical gray and white matter volume in the macaque. Biol Psychiatry 57:83–90. doi:10.1016/j.biopsych.2004.10.014

66. Šestan N, Rakic P, Donoghue MJ (2001) Independent parcellation of the embryonic visual cortex and thalamus revealed by combinatorial Eph/ephrin gene expression. Curr Biol 11:39–43. doi:10.1016/S0960-9822(00)00043-9

67. Sharma J, Angelucci A, Sur M (2000) Induction of visual orientation modules in auditory cortex. Nature 404:841–847. doi:10.1038/35009043

68. Shimogori T, Grove EA (2005) Fibroblast growth factor 8 regulates neocortical guidance of area-specific thalamic innervation.

J Neurosci 25:6550–6560. doi:10.1523/JNEUROSCI.0453-05.2005

69. Shipp S (2003) The functional logic of cortico-pulvinar connections. Philos Trans R Soc Lond B Biol Sci 358:1605–1624. doi:10.1098/rstb.2002.1213

70. Siris SG, Bench C (2003) Depression and schizophrenia. In: Hirsch SR, Weinberger DR (eds) schizophrenia. Blackwell Publishing, Oxford, pp 142–167

71. Skottun BC, Skoyles JR (2008) A few remarks on attention and magnocellular deficits in schizophrenia. Neurosci Biobehav Rev 32:118–122. doi:10.1016/j.neubiorev.2007.06.002

72. Slaghuis WL (1998) Contrast sensitivity for stationary and drifting spatial frequency gratings in positive- and negative-symptom schizophrenia. J Abnorm Psychol 107:49–62. doi:10.1037/0021-843X.107.1.49

73. Stockmeier CA, Mahajan GJ, Konick LC, Overholser JC, Jurjus GJ, Meltzer HY et al (2004) Cellular changes in the postmortem hippocampus in major depression. Biol Psychiatry 56:640–650. doi:10.1016/j.biopsych.2004.08.022

74. Sullivan PR, Kuten J, Atkinson MS, Angevine JB Jr, Yakovlev PI (1958) Cell count in the lateral geniculate nucleus of man. Neurology 8:566–567

75. Sur M, Angelucci A, Sharma J (1999) Rewiring cortex: the role of patterned activity in development and plasticity of neocortical circuits. J Neurobiol 41:33–43. doi:10.1002/(SICI)1097-4695(199910)41:1<33::AID-NEU6>3.0.CO;2-1

76. Sweet RA, Dorph-Petersen K-A, Lewis DA (2005) Mapping auditory core, lateral belt, and parabelt cortices in the human superior temporal gyrus. J Comp Neurol 491:270–289. doi:10.1002/cne.20702

77. Torrey EF, Webster M, Knable M, Johnston N, Yolken RH (2000) The stanley foundation brain collection and neuropathology consortium. Schizophr Res 44:151–155. doi:10.1016/S0920-9964(99)00192-9

78. Ungerleider LG, Mishkin M (1982) Two cortical visual systems. In: Ingle DJ, Goodale MS, Mansfield RJW (eds) Analysis of visual behavior. MIT Press, Cambridge, pp 549–586

79. Van Essen DC, Gallant JL (1994) Neural mechanisms of form and motion processing in the primate visual system. Neuron 13:1–10. doi:10.1016/0896-6273(94)90455-3

80. von Melchner L, Pallas SL, Sur M (2000) Visual behaviour mediated by retinal projections directed to the auditory pathway. Nature 404:871–876. doi:10.1038/35009102

81. West MJ, Slomianka L, Gundersen HJG (1991) Unbiased stereological estimation of the total number of neurons in the subdivisions of the rat hippocampus using the optical fractionator. Anat Rec 231:482–497. doi:10.1002/ar.1092310411

82. Young KA, Holcomb LA, Yazdani U, Hicks PB, German DC (2004) Elevated neuron number in the limbic thalamus in major depression. Am J Psychiatry 161:1270–1277. doi:10.1176/appi.ajp.161.7.1270